

RESEARCH ARTICLE

A Self-Sealing Modular Microfluidic System Using PDMS Blocks With Magnetic Connections

RAFAEL ECKER¹, (Member, IEEE), TINA MITTERAMSKOGLER¹, (Member, IEEE),
MANUEL LANGWIESNER, ANDREAS FUCHSLUGER¹, (Member, IEEE),
MARCUS A. HINTERMÜLLER¹, AND BERNHARD JAKOBY¹, (Fellow, IEEE)

Institute for Microelectronics and Microsensors, Johannes Kepler University Linz, 4040 Linz, Austria

Corresponding author: Rafael Ecker (rafael.ecker@jku.at)

This work was supported in part by the COMET-K2 “Center for Symbiotic Mechatronics” of the Linz Center for Mechatronics (LCM) funded by the Austrian Federal Government and the Federal State of Upper Austria, and in part by the Austrian Research Promotion Agency (FFG) Project AUTOMATE under Project 890068.

ABSTRACT A modular microfluidic system can be used to quickly set up an individually adaptable microfluidic network by linking and delinking different functional building blocks. We present a convenient and reliable connection technology, which is based on magnets and casted O-ring-like structures leading to a sealed connection without the need of additional sealing materials. Based on an improved, previously presented fabrication technology, modular microfluidic polydimethylsiloxane (PDMS) blocks using a polyurethane (PU) mold, 3D printed acrylonitrile butadiene styrene (ABS) channel structures and a magnetic connection system in combination with a casted O-ring link, featuring various integration technologies have now been designed and experimentally evaluated. In particular, this paper will address the realization of directional valves, reciprocating pumps, finger pumps, directly-cast check- and Tesla-valves, fluidic flow sensors, fluidic mixers, commercial valves, and various sensors. By using different measurement setups, the feasibility of these devices is demonstrated. Moreover, limitations and issues encountered during fabrication as well as future work are discussed.

INDEX TERMS Magnetic connection, fabrication technology, flow sensor, fluidic mixer, modular microfluidics, PDMS, PU mold, pumps, valves.

I. INTRODUCTION

The field of microfluidics has gained increasing interest over the last years and has become a standard approach to handle small amount of liquids. Microfluidic chips are applied in various fields ranging from biological sensing, chemical analysis, medicine, science, food industry, and environmental engineering [1], [2], [3], [4], [5], [6]. Compared to liquids at the macroscopic scale for which body forces like gravitation play a major role, microfluidics is dominated by surface forces and associated surface energies. Because of the typically encountered small Reynolds numbers, microfluidic flow is dominated by viscous forces and thus can be assumed to be laminar, which leads to a more predictable and controllable liquid behavior compared to macroscopic systems [7].

The associate editor coordinating the review of this manuscript and approving it for publication was Yassine Malch¹.

Due to the wide range of applications for microfluidic chips, the availability of tools for developing, testing and prototyping designs and design ideas is of particular importance. Current state of the art fabrication techniques like hot embossing, injection molding, laser ablation, 3D printing, and focused ion beam machining enable the fabrication of high-quality microfluidic chips [8]. However, the obtained chips cannot be easily adapted and adjusted by the users themselves [9]. The greatest advantage of a modular system lies in the reusability and exchangeability of individual blocks. While for a commonly used specific single chip, it is not possible to change parts of the implemented microfluidic network, a modular system allows the exchange and rearrangement of components by splitting up the network into different parts separated in different blocks or modules. Applications requiring disposable components (e.g., for hygienic reasons), biology, chemistry, medicine, food

companies, science, and teaching are only a few of the many fields that could benefit from such a modular microfluidic system [4], [9], [10], [11], [12].

One intuitive approach to achieve such a modular system is to utilize the design of LEGO® blocks. Owens et al. [5] micromilled microchannels into the faces of commercially available LEGO® bricks and sealed them with a polyethylene film, whereas Vittayarukkul et al. [6] presented PDMS replica with incorporated microchannels. Similarly, a puzzle-like interlocking structure can be used which relies on the interlocking design for sealed connections [13]. Both approaches have the advantage that the used components can be combined in any way. Yet, a baseplate is necessary to warrant the stability of the entire arrangement.

It has been shown that the modular approach works also for open microfluidic networks [14] and three-dimensional networks [15], [16], [17]. When using PDMS as base material, even whole organ-on-a-chip systems can be fabricated [18], [19]. However, a general drawback of modular approaches is the need for sealed interconnections in between the individual blocks. While form-fit structures can be sufficient to obtain sealed connections for low pressures [5], [6], [14], [20], [21], additional components like glass tubes [19], O-rings [5], [22], [23], [24], or a bottom plate [25] have to be used.

A permanent magnet-based connecting mechanism was also used in earlier works [24], [26]. Both 3D printed and PMDS-based modules were, e.g., presented by Yuen [24]. Here, an additional sealing medium (square O-ring or Kapton polyimide adhesive tape) was required for the employed magnetic connections. The placement of the magnets, due to their orientation, requires connection to a module port featuring the suitable opposite magnetic pole, which is not the case for our system as described below. In [26], a PDMS gasket and an external magnetic connector module (magnetic clamp) are additionally needed to connect the modules.

In contrast to existing approaches, we present modular microfluidic blocks (MMBs) based on PDMS that provide reversible, self-sealing and self-aligning connections using a mechanism that is based on magnetic forces. Rather than having dedicated connector modules [18], [26], we employ a symmetric block design allowing blocks with up to four liquid in- or outlets in the present configuration. Leak-free operation for pressures up to 175 kPa is ensured due to an O-ring-inspired protrusion directly included in the PDMS MMB around the connection interface, without the need of any extra components.

II. CONNECTION SYSTEM

To enable a simple and flexible connection of two arbitrary modular microfluidic blocks (MMBs), a connection system based on neodymium permanent magnets, which are directly integrated into the MMB, is used. It is important that the magnets are glued into the MMB in a properly aligned manner. In Fig. 1a the orientation of the magnetic moment \vec{m} associated with each magnet is indicated. With this arrangement

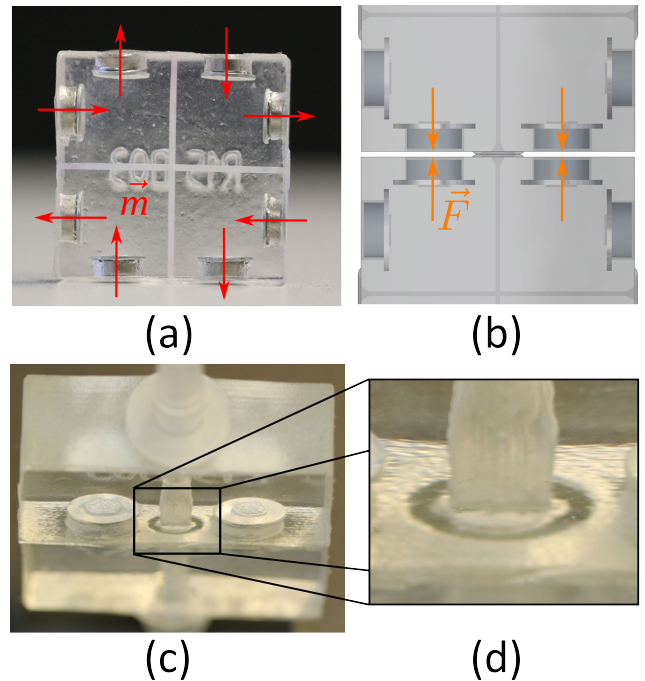


FIGURE 1. Principle of the connection system. a) Modular microfluidic block with shown arrangement of the magnets on each port. The size of the MMB is 30 mm × 30 mm × 10 mm. b) Magnetic force during connection to press the O-ring-like structures together to achieve a sealed connection. c) Two connected blocks with visible connection surface. Width of the half MMB is 30 mm d) Detailed view of the sealing surface.

of the magnets it is possible to connect every connection interface of any MMB with every other one. If two connection interfaces of MMBs get in the nearfield of each other, the magnetic forces \vec{F} automatically align the interfaces properly and connect the MMBs securely. The O-ring-like structures which are present at each connection interface due to the casting process, protrude a bit from the surface (see Fig. 1). Upon connection, two of these O-ring-like structures are pressed together due to these forces exerted by the attracting magnets (Fig. 1b) and establish a sealed interface. Because the channels always start or end in the center of the O-ring-like structures, a sealed connection between the channels of the two connected MMBs is established. Because of the transparency of PDMS, it is possible to observe the sealing interface of two connected MMBs (Fig. 1c and Fig. 1d).

The easiest way to delink the MMBs is to hold one and tilt the other one up or down and pull a bit at the same time. With the current square design of the MMBs a maximum of four ports per MMB are possible. If more ports are necessary, the principle could be extended to hexagonal geometries with six ports or also it should be possible to create two ports per interface using three magnets.

III. MATERIALS

The aim from the very beginning was to produce a transparent module to ensure the visibility of the test fluids in the channel structures. The first tests showed that, in order to create a leak-free connection interface, it is mandatory to have a rather smooth surface at the sealing surface. Therefore, 3D

printing of the MMBs with a filament-based printer or other methods such as using laser engraved polymethyl methacrylate (PMMA) plates with a top plate to seal the block, e.g. as shown in [27], at least need an additional quite complex smoothing step of the sealing surfaces. Furthermore, there is a decisive disadvantage when the MMBs are made out of a hard material, since in order to seal the connection, an additional flexible component, usually an O-ring, is required. This part must be inserted during each connection operation.

Taking into account these circumstances, the choice of the material of the MMBs fell on the well-known PDMS. Disadvantageously, the use of PDMS as material requires a mold. However, the use of a casting process allows the simple integration of external components already during the molding step and therefore also complex outer geometries (such as the placeholders for the magnets, O-rings, etc.) of the MMB can be realized in a single molding step. Additionally, the use of PDMS as a material allows for multiple mold reuses, which opens up the opportunity of mass production. The ability to replicate shapes at the nanoscale is another benefit of PDMS. On the downside, PDMS absorbs different kinds of molecules and starts to swell. The evaporation of different kind of fluids e.g. water through PDMS is another challenge and may potentially lead to issues in long term experiments [28].

Such complex outer geometries like the sealing interface require an associated negatively shaped mold. A template is required to fabricate the mold, which itself has to be fabricated out of a very flexible material in order to enable the removal of the template from the mold. To be able to produce almost any shape with high accuracy, the template is printed with a 3D printer (Stratasys, Objet30 Pro) out of resin (Stratasys, VeroBlack).

After the definition of the materials for the MMB (PDMS) and the template (VeroBlack), the task was to find a flexible and castable material for the mold. Due to the fact that some of the tested materials adhered very well to each other, we also considered the use of a separating agent. Because of the extra step in fabrication, it is desired to limit the use of a separating agent to the fabrication of the mold solely, where the extra step is not so critical, because one mold can be used for the production of several MMBs.

Tests have shown that the material combination of a polyurethane (PU) mold, using the separating agent only for the mold fabrication, with both selected materials (PDMS for the MMB and VeroBlack for the template) work very well. Therefore, PU is used as material for fabrication of the mold. In Fig. 2 an overview of the main parts, their outline and the selected materials is given. In Table 1 the different tested material combinations to determine the mold material are summarized.

IV. FABRICATION

In this section every step of the fabrication procedure is illustrated and discussed starting with the fabrication of the reusable template which is needed for the fabrication of the

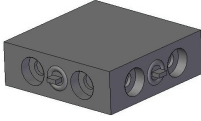
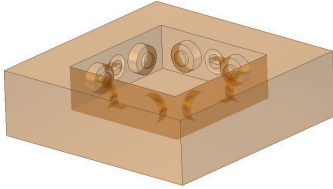
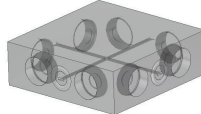
Part	Outline	Material
Template		VeroBlack (3D printer material)
Mold		Polyurethane (PU)
MMB		PDMS

FIGURE 2. Overview of the main parts and the selected materials.

reusable PU mold, which again is needed for casting the MMBs. The basic and preliminary fabrication steps were previously shown in our conference paper [29], went through some final improvements and are described in detail in the following sections.

A. TEMPLATE

The template with the outer contour of the MMB is first designed in a CAD program with dimensions as shown in Fig. 3 and then 3D printed using the mentioned printer and material.

The side walls (Fig. 3 green marked areas) have an angle (slope) of 2° in order to compensate the different thermal expansions of the fully PU-filled bottom and the top of the PU mold during the curing of the PDMS in the mold at high temperatures. This makes it possible to fabricate MMBs with almost perfectly vertical walls. Cylindrical cutouts (gray marked areas in Fig. 3) are provided as placeholders for the neodymium permanent magnets used for the magnetic connection. To fix the magnets in the PDMS modules, they are glued to washers featuring a larger diameter. Doing so, in the final MMB, the outer portion of the washer is fully embedded in the PDMS providing a form-fitting reliably mounting of the magnet/washer arrangement. Respective cutouts for washer and magnet thus need to be provided in the template (Fig. 3 orange marked areas: washer location, grey marked areas: magnet location).

The yellow marked cuboids in Fig. 3 serve as placeholders for the mounting of the negative channel structures in the PU mold and hence are the ports of the later MMB. Around these cubes, embossed structures looking like a half O-ring (blue marked in Fig. 3) are placed. These structures serve as a sealing surface in the later casted MMB.

TABLE 1. Compatibility of mold materials with the template and the modular microfluidic blocks (MMBs) materials.

Materials for MMB/ Template	VeroBlack ^b (template)		PDMS ^a (MMB)
	Without separating agent	With epoxy coating ^c and separating agent ^d	
PDMS ^a	N.A. (MMB molding impossible)	N.A. (MMB molding impossible)	Cannot be molded without disintegration
PU ^e	Molding of straight surfaces possible, yet detailed structures are not possible	Molding is possible	Molding is possible, curing of PDMS at high temperatures is necessary
SF45-RTV2 ^f	Molding of straight surfaces possible, yet detailed structures are not possible	Molding is possible	Cannot be molded without disintegration
RT 622 A/B ^g	Molding is possible	Not tested	Cannot be molded without disintegration

^aSylgard, 184 silicone elastomer kit; ^bStratasys, VeroBlack, ^cR&G Faserverbundwerkstoffe GmbH, Epoxy Resin HT 2 and Hardener HT 2; ^dHenkel, Loctite LB 8192; ^eBiresin®, U1404 Comp. A and U1404 Comp. B; ^fSilikonfabrik, SF45-RTV2; ^gElastosil®, RT 622 A/B;

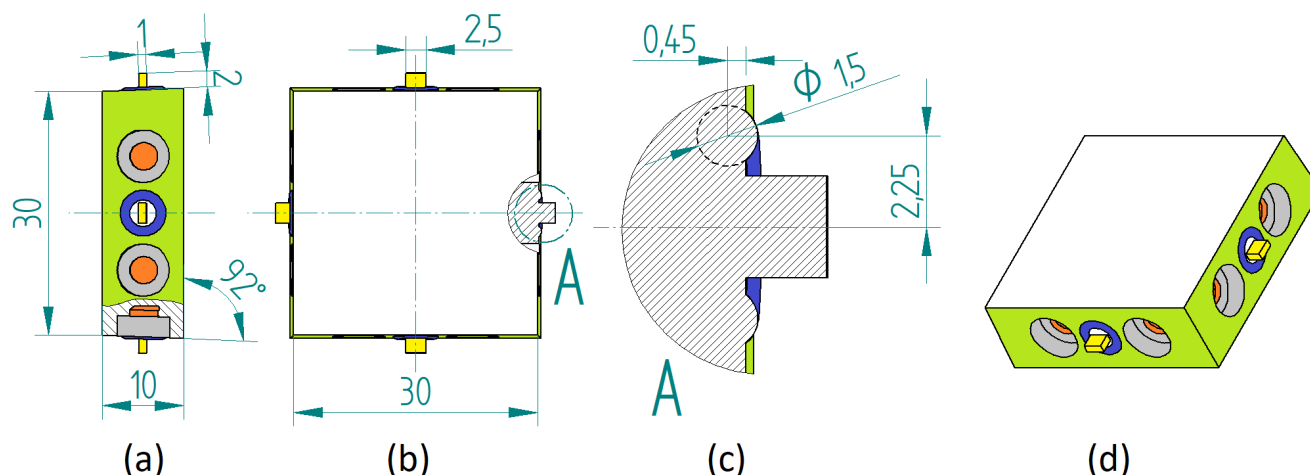


FIGURE 3. Dimensions of the template with marked surfaces for the special parts. (a) Side view, (b) top view, (c) detailed view of the sealing interface, (d) 3D view. Green marked - side walls, grey marked - cutouts for magnets, orange marked - cutouts for washer mounting, yellow marked - placeholder for the channel structures, blue marked - O-ring-like structures as sealing interface.

B. PU MOLD

The main fabrication steps of the PU mold are shown in Fig. 4. We start with the described template (black in Fig. 4a) from which the support structure (associated with the design used for 3D printing) is removed with water after the printing process. The template is first dried and afterwards coated with low-viscosity two-component epoxy resin (R&G Faserverbundwerkstoffe GmbH, epoxy resin HT 2 and hardener HT 2) using a common fine brush (Fig. 4b). For curing the epoxy resin coating, the template is put in the oven at 55 °C for 5 h, see Fig. 4c. This coating, which leads to a smooth surface, in combination with an additional spray coated polytetrafluoroethylene (PTFE) separating agent (Henkel, Loctite LB 8192, see Fig. 4d) enables the subsequent removal of the template out of the PU mold.

A reusable and demountable box is built out of 1.5 mm thick laser cut PMMA plates with the inner dimensions of about 50 mm x 50 mm x 40 mm. The height is needed to accommodate the later expansion of the PU mass during evacuation. To enable the filling of the box, the top is not closed. In the next step (Fig. 4e) the template is glued to

the center of the bottom plate of the PMMA box using a double-sided adhesive foil (Aslan, DK 4). It is important that the template is aligned such that the slopes of the sidewalls are correctly aligned, i.e. that they are tapered from the bottom upwards.

As base material for the mold, a castable PU (Biresin®, U1404 Comp. A and U1404 Comp. B) is used. For preparation components A and B are mixed together using a weight ratio of 8:10 (Comp. A: Comp. B.). The next steps have to happen quite fast, because the pot life of the mixture is only about 25 minutes at room temperature. As a next step, the PU is poured into the PMMA box until the template is covered with about 5 mm PU on top (Fig. 4f). The box is directly put into the vacuum desiccator (Fig. 4g) afterwards for about 15 min, to remove all air bubbles and other air which otherwise would remain in the cutouts. For faster curing of the PU, it is put into the oven at 55 °C for 5 h, see Fig. 4h.

As a final step after cooling down to room temperature, the PMMA box and the template are removed out of the PU mold (Fig. 4i). To do this, first the side walls of the demountable box are tilted to the side at the top, as the PU then slowly

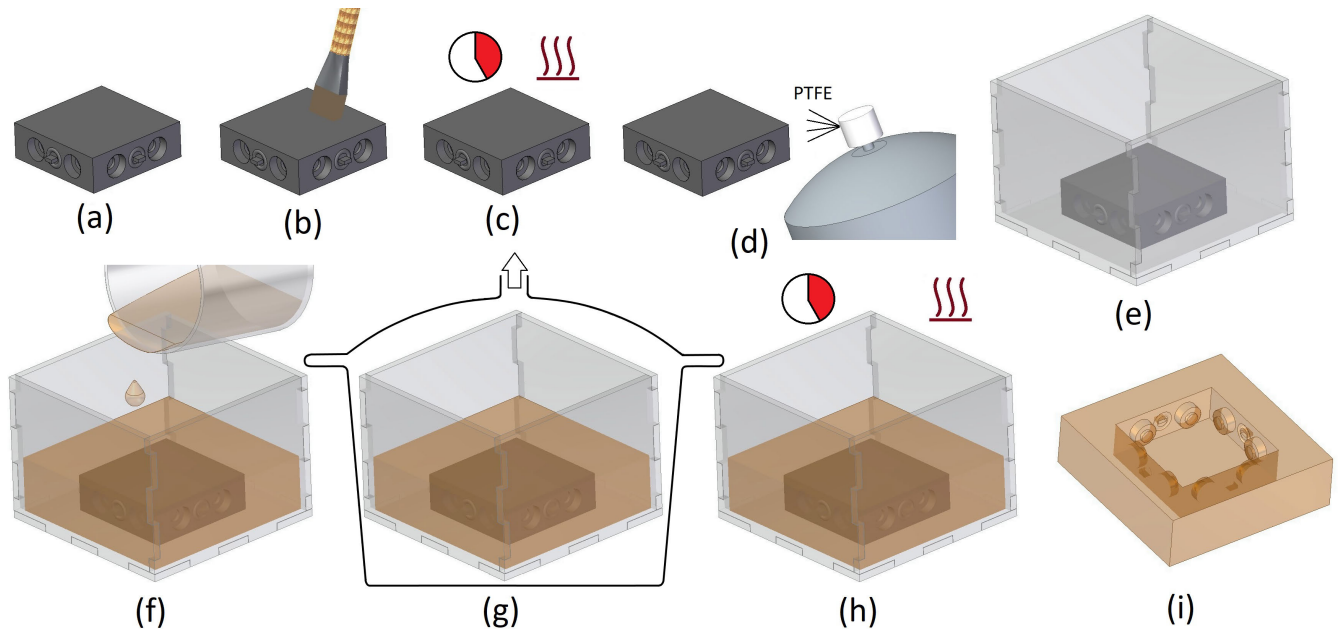


FIGURE 4. Fabrication procedure of the PU mold [23]. a) 3D printing of the template and removing support structure. b) Coating of the template with low viscosity epoxy resin using a common brush. c) Curing of the epoxy resin in the oven at 55 °C for 5 h. d) Spray coating the template with a PTFE layer. e) Placement and fixing of the template into a demountable PMMA box using a double-adhesive foil. f) PU preparation and casting. g) Air bubble removal by evacuation for 15 min. h) Curing of the PU into the oven at 55 °C for 5 h. i) Removal of the PMMA box and the template, final PU mold.

detaches from the walls. Then the same is done with the bottom PMMA plate afterwards. Since the cured PU is very flexible, the template can be removed by pressing the PU mold at the interfaces and then lifting it out. To enable the curing of the PDMS, the PU mold has to rest for at least 3 days allowing the remaining curing agents to escape. Additionally, the PU mold is cleaned with isopropanol before every use.

C. CHANNEL STRUCTURES (NEGATIVES)

In order to fabricate the MMBs with different fluidic functions using a PDMS casting process, in addition to the mold already described, negatives of the desired channel structures are required to prevent the desired channels being filled during the casting process. After the casting process, these negatives of the channel structures must be removed from the PDMS MMB so that the channels are free and the MMB works as desired. For simple, straight channels, the associated negatives can most often simply be removed by pulling them out of the cast MMB (and they can even be reused in this case). For more complex channel geometries, however, materials that can be chemically dissolved have to be selected for these negatives. Acrylonitrile butadiene styrene (ABS) in combination with acetone as solvent fulfills exactly the desired property and has previously been successfully used for the desired application [30]. Another key advantage of using ABS as material for the channel negatives is that it is one of the most widely used materials for fused deposition modeling (FDM) 3D printing [7]. The material itself is therefore readily available on the market. Due to the use of an 3D printer (Ultimaker, 2+ Extended), the fabrication of almost any 3D (negative) channel shape is possible. On the down-

side, the use of an FDM printer limits the channel geometries in size downwards, due to the used nozzle diameter (400 μm) and the accuracy of the printer itself. With the used setup, it was possible to print channel structures with the smallest dimensions of 300 μm width and 60 μm height.

In order to keep the negatives in the desired position during the later casting process of the PDMS they are printed 2 mm longer at the later ports and inserted into the placeholder of the PU mold (Fig. 3 and Fig. 5a).

D. MODULAR MICROFLUIDIC PDMS BLOCK

Fig. 5 shows the main fabrication steps of a PDMS MMB. After cleaning the PU mold using isopropanol and drying it again the already printed ABS channel negative is inserted into the placeholders of the reusable PU mold (Fig. 5a). As next step (Fig. 5b) the washers, to which the magnets will be glued later on, featuring an outer diameter of 9 mm and 3.2 mm inner diameter (standard washers for M3 screws) are placed onto the holders of those sides of the PU mold where a port is provided. Because of the special shape of the holders (see Fig. 3a orange marked area) the washers remain in place even during movements and pouring. Experiments showed that it is virtually impossible to glue the permanent magnets directly to the PDMS, due to its low surface energy, which is why the washers were introduced in the design. The washers themselves are casted into the PDMS MMB yielding a form-fitting connection.

To cast one MMB with the dimensions of 30 mm x 30 mm x 10 mm, about 12 g PDMS (Dow Silicones Deutschland GmbH, Sylgard™ Silicone Elastomer Kit) is mixed according to manufacturer specifications using a weight ratio of

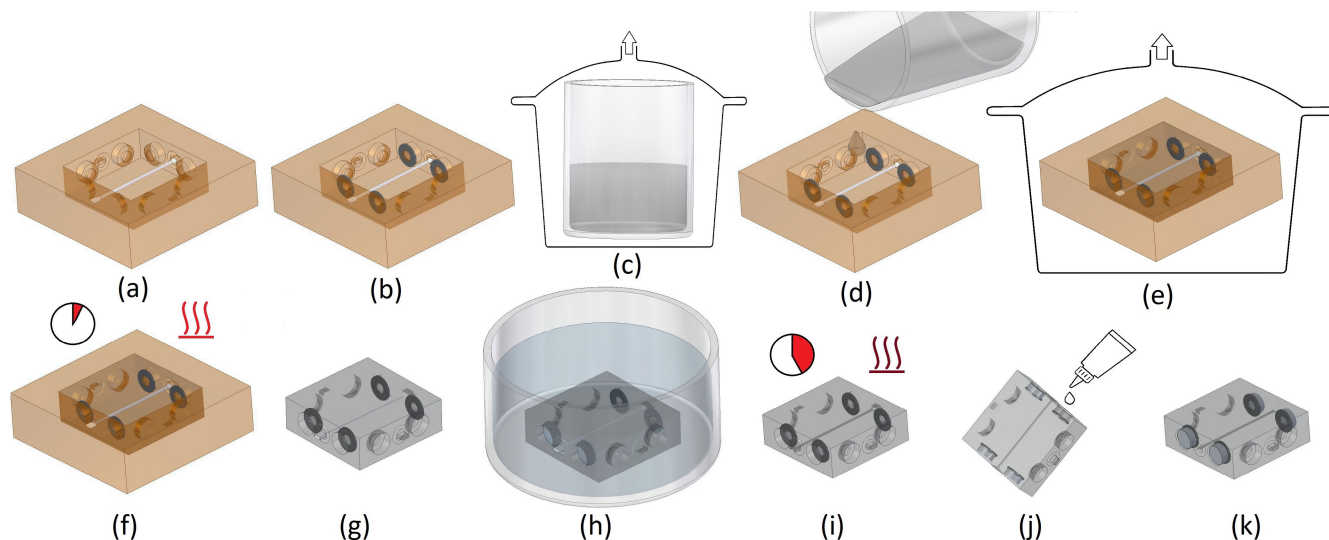


FIGURE 5. Fabrication procedure of the PMMA MMB [23]. a) Inserting the printed channel structures into the placeholders of the PU mold. b) Placing the washers onto the holders of each used connection port. c) Mixing and degassing of the PDMS base material. d) Casting of the PDMS. e) Bubble removing by evacuation. f) Curing of the casted MMB. g) Demolding of the PDMS MMB. h) Dissolving of the ABS channel structure in acetone. i) Removing of the absorbed acetone. j) Adhering the magnet to the washers using a glue. k) Fabricated and usable PDMS MMB.

10:1 (base to curing agent). The mixture is afterwards put into the vacuum desiccator (Fig. 5c) for about 15 min for degassing (before pouring it into the mold). As shown in Fig. 5d, next the PDMS is poured into the PU mold until the mold is brimful. To remove trapped gas which otherwise will remain in the PU mold and under to channel structure the filled PU mold is evacuated once more, see Fig. 5e. The PDMS is then cured in the oven at 90 °C for 1 h (Fig. 5f). In a series of initial experiments, it was found that such a high curing temperature is needed to avoid curing problems at the PDMS/PU interface.

After cooling down, the PDMS MMB is removed out of the PU mold (Fig. 5g), which is easily possible because both the PDMS and the PU mold are quite flexible. As already described, after the casting process, the ABS negative, which is still embedded into the MMB, has to be dissolved using acetone (or pulled out in simpler cases, as described above). To do so, the MMB is put into acetone for typically two days (Fig. 5h) and afterwards additionally flushed with acetone, which removes the remaining ABS. During the time the PDMS stays in acetone it absorbs some of it and therefore swells. To remove the absorbed acetone, the MMB is afterwards placed into the oven at 55 °C for 5 h (Fig. 5i).

Due to the casting process in combination with the evacuation, the washers are covered with a thin layer of PDMS on the side of the cutout for the magnet. Therefore, before the neodymium permanent magnets (Wecraft GmbH, S-06-02-N), with a diameter of 6 mm and a height of 2 mm, are attached to the washers using a glue (Loctite®, 4850), see Fig. 5j, this layer has to be removed using a scalpel. Finally, the overlaying PDMS at the top and the former place holders is cut off using a wire cutter. The fabricated and usable PDMS MMB is shown in Fig. 5k.

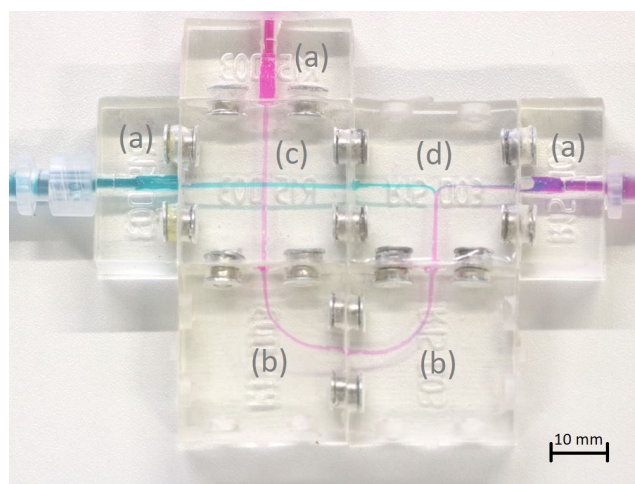


FIGURE 6. Modular microfluidic network using only connection MMBs. a) Start or end blocks. b) Curves. c) Crossover block. d) Three-way block.

V. FABRICATED MODULAR MICROFLUIDIC BLOCKS (DEMONSTRATORS)

A. CONNECTION BLOCKS, ROUTING AND MIXING

Start and end blocks (see Fig. 6a) are made as a half block (dimensions 30 × 15 × 10 mm) and therefore require their own PU mold. The “removed” half is used to host a Luer connector, which allows easy and standardized connection to external syringes, tubes, valves, pumps, and much more.

The most fundamental MMBs are simple “through” connections. The basic connection blocks are straight, curve, crossover, three-way, and four-way connectors. Fig. 6 shows a modular microfluidic network (MMN) build up using only connection blocks with colored water in the channels to make them more visible. To fabricate the crossover MMB, two

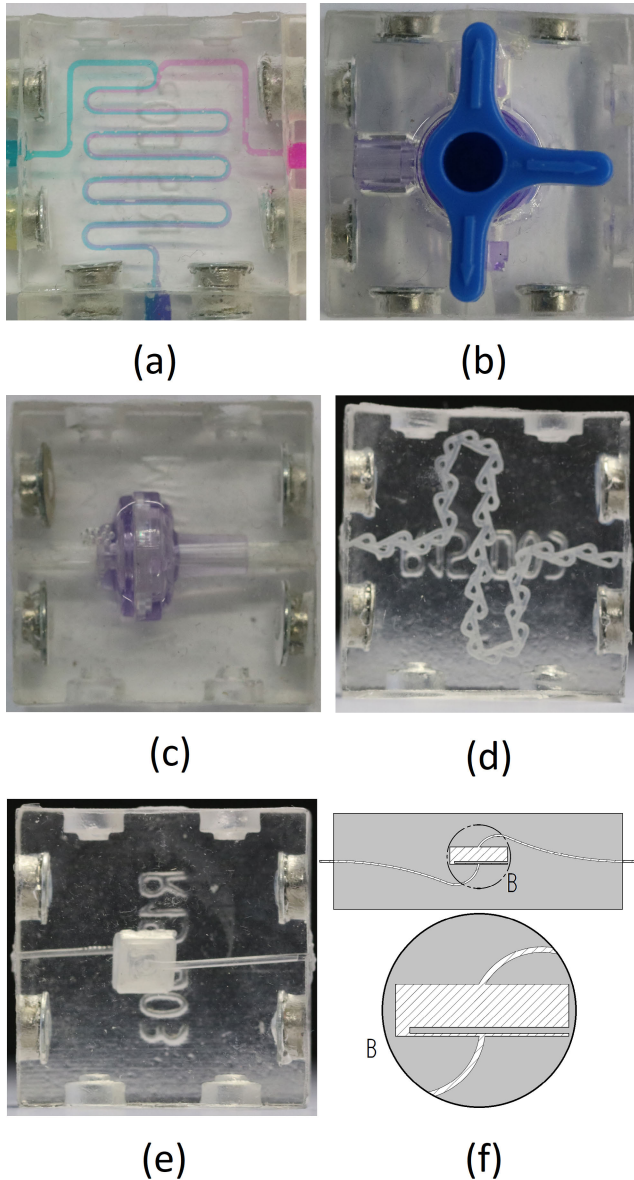


FIGURE 7. Fabricated mixer and valve MMBs. a) Fluidic mixer with colored ink to see the mixing because of diffusion. b) Integrated commercial three-way-valve. c) Integrated commercial nonreturn valve. d) Tesla valve. e) PDMS only nonreturn valve. f) Sectional view of the channel structure of the PDMS only nonreturn valve. The PDMS is gray marked in this view. The size of each MMB is 30 mm × 30 mm × 10 mm.

straight channels are used, one about 1 mm longer than the mold. Both are inserted into the mold (Fig. 5a), because one is a bit too long it bends upwards or downwards. It is important that the bend direction is specified such that both channels do not touch each other.

Flows in the microfluidic range are virtually always laminar [31], consequently the mixing of two different fluids happens mainly due to diffusion, which is a slow process [32]. To enable the mixing of two fluids, channel structures with long interfaces and small dimensions as well as low flow rates are necessary. A fabricated mixer which mixes colored water is shown in Fig. 7a. Such a device is well-suited to demon-

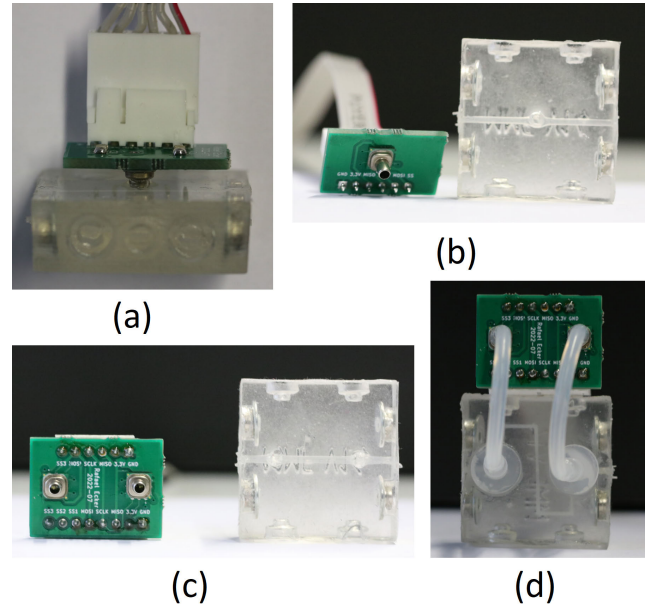


FIGURE 8. Pressure sensor and flow sensor MMBs. a) Pressure sensor plugged into the corresponding MMB. b) Circuit board with the pressure sensor separated from the MMB. c) Unplugged flow sensor circuit board using two pressure sensors for measurement and the corresponding MMB. d) Flow sensor MMB using flexible connection tubes to eliminate the sealing issues. The size of each MMB 30 mm × 30 mm × 10 mm.

strate the mixing behavior at the microscale. The different stages of the diffusion process are visible clearly and even at the end of the structure the different colors are visible.

B. VALVES

In order to be able to control the flows in an MMN, different valves are required. The easiest way to build MMBs with valve functionality is to embed commercially available ones directly into the MMB during the casting process. The connection between the valve and the connection interface of the MMB is again achieved using printed ABS channel structures. Because many of the plastic parts of the standard valves also dissolve in acetone, in this case only straight channels are used enabling removal using the pulling-out method as outlined above. Using this technique, three-way valves (Teqler®, three-way stopcock) and nonreturn valves (BD, check valve) for Luer connections were integrated successfully (see Fig. 7b and 7c). It is possible to integrate virtually every device, as long as the dimensions of the valve fit into the MMB.

The direct fabrication of fully PDMS based valves is also possible. A so-called Tesla valve is geometrically designed to allow the fluids to flow through easily in one direction and to restrict the other flow direction [33]. Therefore, the flow resistance is different between the forward and reverse flow directions. A fabricated Tesla valve is shown in Fig. 7d.

To build up a castable PDMS nonreturn valve (Fig. 7e) we printed a special channel structure (Fig. 7f). After fabrication, a small chamber remains in the MMB with an input on top and an output on the bottom. A small moveable PDMS wall, which is loose on three sides, closes the

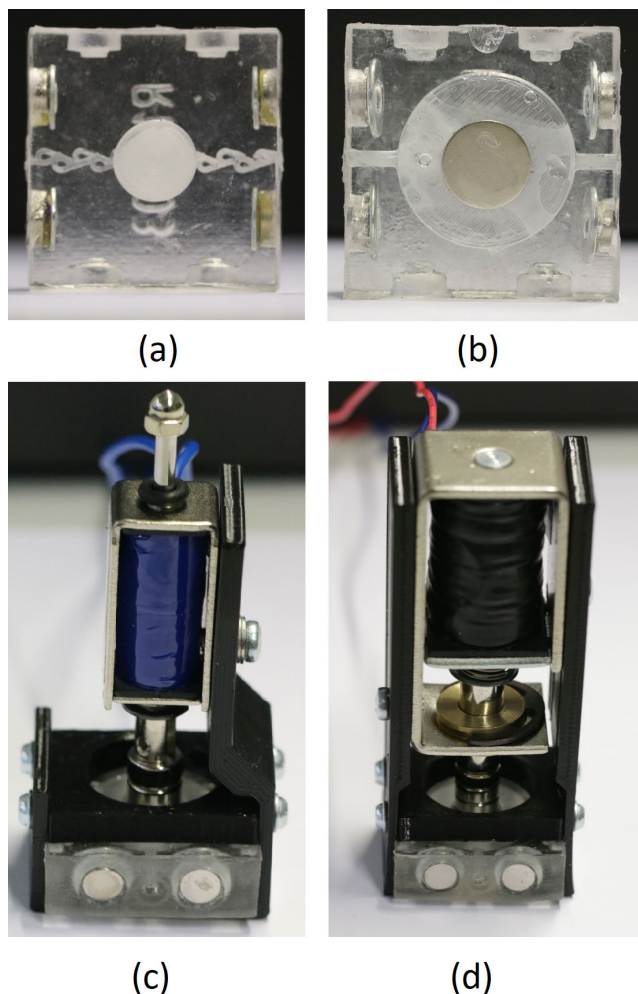


FIGURE 9. Diaphragm pumps MMBs. a) Finger pump with integrated Tesla valves. b) MMB with integrated magnet for pumping with the electromagnetic actuators (EAs). c) Pump with small EA, fixed onto the MMB with a 3D printed mounting structure. d) Diaphragm pump for higher pressures using a bigger EA. The size of each MMB is 30 mm × 30 mm × 10 mm.

output in one direction if the flow rate is high enough. In the other flow direction, the PDMS wall (gray small strip on the bottom of the white chamber in Fig. 7f) cannot block the output, because the distance between the wall and the output is too high. Due to the limited print size, the wall has to move a bit (about 100 μm) to close the output. In this design, the required flow rate to close this valve is quite high, compared to smaller microfluidic chips (in the range of 500 μl/min).

C. SENSORS

Sensors are required to determine the fluid and flow properties of an MMN at the desired points. For liquid-based systems, the two most important variables are the pressure and the flow velocity. Therefore, as a first step a pressure sensor MMB was fabricated, see Fig. 8a and 8b. The measurement is performed by a commercially available pressure

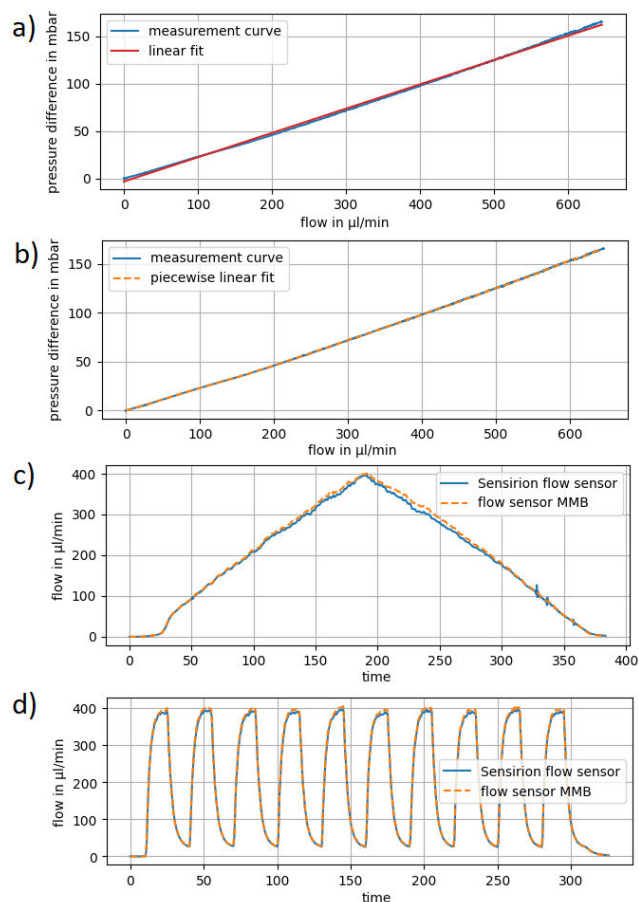


FIGURE 10. Calibrations curves and measurements using the flow sensor MMB and a commercial flow sensor. a) Measured calibration curve with the corresponding linear fit. b) Measured calibration curve and its piecewise linear fit. c) and d) Example measurements using the commercial and the fabricated flow sensor for comparison.

sensor (Honeywell, MPRLS0030PG0000SA) mounted on a custom designed circuit board (fabricated by JCLPCB Ltd.). The sensor is plugged into a port on top of a specially designed MMB. In future it is planned to directly integrate the sensor with the circuit board into the PDMS MMB during the fabrication process.

Based on a differential pressure measurement between two sides of a fluidic resistor, it is possible to build a flow sensor MMB, which is shown in Fig. 8c. The flow velocity v can be calculated ideally from the measured pressure difference Δp and the flow resistance R_f using

$$v = \frac{\Delta p}{R_f} \tag{1}$$

Because PDMS is flexible, the channel geometry changes a bit if the pressure varies. Consequently, the flow resistance R_f of a particular channel segment depends on the applied pressure difference Δp . The behavior is therefore not ideally linear and was calibrated using an external flow sensor (Sensirion, SLI-1000).

To realize the flow sensor MMB, two pressure sensors (Honeywell, MPRLS0030PG0000SA) are mounted onto a printed circuit board (PCB) and again plugged into a specially designed MMB (see Fig. 8c and 8d). To achieve a sealed interface between the two sensors, which, by virtue of the PCB setup, are arranged at a pre-defined distance, and the two MMB plugs on top, it is quite important to work exactly and with small tolerances. The flow sensor MMB in Fig. 8d relaxes this challenge by using flexible connection tubes. The direct integration of the sensors with the circuit board will automatically eliminate this problem.

For the readout of the measurement data from the sensors, a microcontroller (Arduino, Nano) in combination with a custom-made circuit board was used. Furthermore, the measured data was displayed on an LCD and transferred to a PC via the serial interface, which enables to store the data permanently and to display them in a diagram.

The integration of many other sensors for characterizing liquids such as viscosity or conductivity sensors is easily possible as long as the sensors fit geometrically into an MMB. Due to the high transparency of PDMS, the opportunity to integrate optical sensors like turbidity sensors, sensors for bubble detection, measurement of oxygen saturation in blood, etc. is also given. If necessary, it would be possible to fabricate geometrically larger MMBs, which cover two, four, or more standard MMBs with an adaptable height.

D. PUMPS

To generate a fluidic flow within the MMN, pumps are required. In combination with the start/end MMBs and the

Luer connector, the use of external pumps is easily possible. The integration of commercially available micropumps directly into the MMB is also possible and straightforward.

Due to the flexibility of PDMS, the fabrication of a diaphragm pump was near at hand. The basic idea here was to fabricate an MMB featuring a reservoir with a thin deformable upper PDMS wall (approx. 1 – 1.5 mm in our design). In combination with two nonreturn valves or Tesla valves, the pumps will work as follows. Reducing the volume in the pump reservoir by pressing on the upper wall would normally lead to a flow at both openings (inlet and outlet respectively) of the reservoir. However, the valve situated at the inlet closes in this case and prevents a backflow. The second valve remains open, which creates a fluidic flow in the desired direction. After releasing the pressure, the upper PDMS wall returns the initial position and generates a negative pressure. Now the situation is exactly reversed and the valve at the outlet is closed. The valve at the input opens and water is sucked into the pump via the inlet. A fabricated pump with manual operation (using, e.g., a finger to press the PDMS MMB) is shown in Fig. 9a. To automate this pump and in addition increase the working speed, a neodymium magnet (Webcraft GmbH, S-10-0.6-STIC or S-10-01-STIC) was integrated into the upper wall (diaphragm) of the pump, see Fig. 9b. At the outside an electromagnetic actuator (EA) is placed, which can move a piston up and down. By placing an

TABLE 2. Leakage test of the connection system.

Number of connected blocks	Pressure where first leakage was notable in kPa	Used blocks
2	195	2 x start/end block
2	200	2 x start/end block
2	195	2 x start/end block
3	190	2 x start/end block, 1 x curve
3	175	2 x start/end block, 1 x curve
3	190	2 x start/end block, 1 x finger pump
3	205	2 x start/end block, 1 x diaphragm pump
3	180	2 x start/end block, 1 x crossover
3	195	2 x start/end block, 1 x Tesla valve
4	210	2 x start/end block, 2 x curve
4	205	2 x start/end block, 1 x curve, 1 x Tesla valve
5	175	2 x start/end block, 2 x curve, 1 x three-way-valve
5	185	2 x start/end block, 1 x curve, 1 x Tesla valve, 1 x crossover
6	175	2 x start/end block, 2 x curve, 1 x Tesla valve, 1 x crossover
6	190	2 x start/end block, 2 x curve, 1 x Tesla valve, 1 x finger pump

additional magnet onto the top of the piston, the connection to the integrated magnet was established. With this system it was possible to displace the diaphragm in both directions, i.e. up and down, maximizing the pumping volume. Two different sizes were fabricated and are shown in Fig. 9c and Fig. 9d.

VI. RESULTS

A. CONNECTION SYSTEM

To evaluate the devised connection system, different MMBs were connected and all ports were closed except for one input and one output. The output was connected to a pressure sensor (Honeywell, ABPMANV030PG2A3) and at the input, water was slowly and manually pressed into the system using a syringe. Doing so, the pressure in the MMN starts to rise. At a specific pressure the system becomes leaky at a connections interface. This pressure is measured and given in Tab. 2 for a different number of devices. Overall, the system stays sealed up to a pressure of at least 175 kPa. For every individual connection this value varies a bit. For bigger MMNs the connection with the lowest value is the limiting one. However, the connections remain sealed up to fairly high pressures which means that, except from these sealing tests, such pressures would have never been reached in any of the other experiments concerning the MMBs functionality. If necessary, an increase of the maximal possible pressure can be achieved, e.g., by using stronger or additional magnets, though.

B. FLOW SENSOR MMB

The function of the fabricated flow sensor MMB is shown by setting different fluidic flows using an external syringe pump (Cellix, ExiGo pump) and simultaneously measuring the actual flow with a commercial flow sensor (Sensirion,

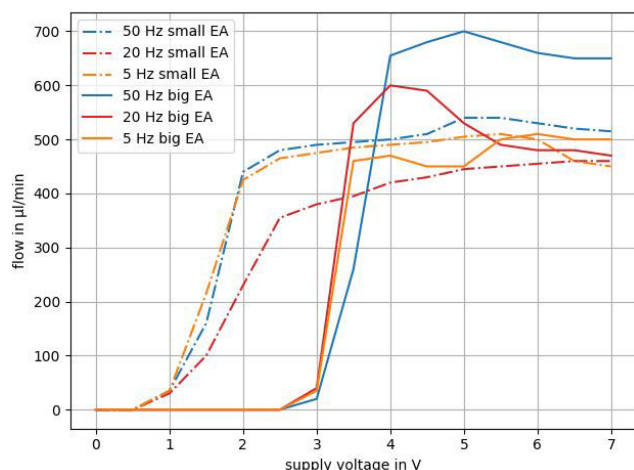


FIGURE 11. Flow rate of the diaphragm pumps with the small and the big EA at different voltages and frequencies.

SLI-1000) and the corresponding differential pressure of the flow sensor MMB. Such a measurement is shown in Fig. 10a (blue curve). According to (1), the mathematical relationship between the flow velocity and the pressure difference in a microfluidic channel with constant flow resistance is approximately linear. The measurement curve (blue curve) in Fig. 10a is fairly linear, but the linear fit (red curve) shows that it is not perfectly linear. The reason for this is the already mentioned elasticity of PDMS causing the flow resistance to depend on the actually present pressure. To compensate this, a piecewise linear fit was used for the calculation of the flow velocity from the pressure difference. Fig. 10b shows the comparison between the measurement curve (blue curve) and the calibration curve (orange dashed curve) of the flow sensor MMB using the piecewise linear fit. The difference between both curves is quite small and therefore the piecewise linear fit function is used for the following measurements. Two sample measurements (see Fig. 10c and Fig. 10d) demonstrate the feasibility of the developed and calibrated flow sensor MMB when compared to the values obtained using the commercial flow sensor.

C. DIAPHRAGM PUMPS

The tests showed that the pumps work reliably up to a frequency of about 50 Hz. When the frequency was increased further, the output flowrate decreased significantly with increasing frequency. This maximum frequency can therefore be used to obtain high flow rates but keeping the pulsation of the output flow small at the same time. We note that due to the elasticity of the PDMS, the pulsation happens to be increasingly attenuated for increasing frequencies. The output flow rate of the two fabricated pumps versus the peak voltage of the pulse width modulated (PWM) signal with a duty cycle of 50 % at different frequencies is shown in Fig. 11.

After overcoming a minimum voltage, the maximum possible flow rate is reached quickly. Further increase of the voltage virtually does not increase the flow rate any further.

The maximal possible output pressure is determined by the spring and its force on the MMB. The increment of the voltage leads to an increase of the output pressure until this maximum. Using different springs, the pressure could be changed to meet different requirements. With the current pumps, the maximum pressures achieved are 150 mbar using the bigger EA and 60 mbar using the smaller EA.

VII. CONCLUSION AND OUTLOOK

In this paper a low-cost fabrication procedure of PDMS MMBs and the required PU mold was shown. Using 3D printed ABS channel structures, as well as the possibility to integrate commercially available devices, enables an enormous flexibility and variety of different possible MMBs.

The devised magnetic connections system offers a self-sealing and self-aligning property, which allows an easy linking and delinking of the MMBs, while at the same time it stays sealed up to fairly high pressures of about 175 kPa. The variety of different fabricated demonstrator MMBs in combination with presented results as well as the outlined possibilities to fabricate further MMBs illustrates a wide field of possible applications.

Future work will focus on the fabrication and integration of more sensors, e.g., optical sensors or actuators. To enable the downscaling of the system using the current fabrication procedure, a high-resolution 3D printer, being able to print a dissolvable polymer, is required. Such a printer is currently not available to our knowledge. Another option might be to use a conventional SU-8 photolithography process to create channels with dimensions in the lower micrometer range. For this purpose, it would be necessary to cast the PDMS MMBs with a cuboid cutout in the center of the block (at the location of the microfluidic channels). A high-precision technology, such as SU-8 photolithography, would have to be used to create the cuboid with the desired channel structure on the bottom, and it then would have to be bonded with the channels side down into the MMB using an oxygen plasma treatment procedure. The connecting systems would remain unchanged in this case.

REFERENCES

- [1] G. Kaur, M. Tomar, and V. Gupta, "Development of a microfluidic electrochemical biosensor: Prospect for point-of-care cholesterol monitoring," *Sens. Actuators B, Chem.*, vol. 261, pp. 460–466, May 2018, doi: [10.1016/j.snb.2018.01.144](https://doi.org/10.1016/j.snb.2018.01.144).
- [2] V. J. Sieben, C. F. A. Floquet, I. R. G. Ogilvie, M. C. Mowlem, and H. Morgan, "Microfluidic colourimetric chemical analysis system: Application to nitrite detection," *Anal. Methods*, vol. 2, no. 5, pp. 484–491, 2010, doi: [10.1039/C002672G](https://doi.org/10.1039/C002672G).
- [3] B. Al Mughairy and H. A. J. Al-Lawati, "Recent analytical advancements in microfluidics using chemiluminescence detection systems for food analysis," *TrAC Trends Anal. Chem.*, vol. 124, Mar. 2020, Art. no. 115802, doi: [10.1016/j.trac.2019.115802](https://doi.org/10.1016/j.trac.2019.115802).
- [4] Y.-Q. Fan, H.-L. Wang, K.-X. Gao, J.-J. Liu, D.-P. Chai, and Y.-J. Zhang, "Applications of modular microfluidics technology," *Chin. J. Anal. Chem.*, vol. 46, no. 12, pp. 1863–1871, Dec. 2018, doi: [10.1016/S1872-2040\(18\)61126-0](https://doi.org/10.1016/S1872-2040(18)61126-0).
- [5] C. E. Owens and A. J. Hart, "High-precision modular microfluidics by micro-milling of interlocking injection-molded blocks," *Lab Chip*, vol. 18, no. 6, pp. 890–901, 2018, doi: [10.1039/C7LC00951H](https://doi.org/10.1039/C7LC00951H).

- [6] K. Vittayarukskul and A. P. Lee, "A truly Lego®-like modular microfluidics platform," *J. Micromech. Microeng.*, vol. 27, no. 3, Jan. 2017, Art. no. 035004, doi: [10.1088/1361-6439/aa53ed](https://doi.org/10.1088/1361-6439/aa53ed).
- [7] H. Bruus, *Theoretical Microfluidics, Illustrated Edition*. New York, NY, USA: Oxford Univ. Press, 2007.
- [8] S. Scott and Z. Ali, "Fabrication methods for microfluidic devices: An overview," *Micromachines*, vol. 12, no. 3, p. 319, Mar. 2021, doi: [10.3390/mi12030319](https://doi.org/10.3390/mi12030319).
- [9] X. Lai, M. Yang, H. Wu, and D. Li, "Modular microfluidics: Current status and future prospects," *Micromachines*, vol. 13, no. 8, p. 1363, Aug. 2022, doi: [10.3390/mi13081363](https://doi.org/10.3390/mi13081363).
- [10] K. A. Shaikh, K. S. Ryu, E. D. Goluch, J.-M. Nam, J. Liu, C. S. Thaxton, T. N. Chiesl, A. E. Barron, Y. Lu, C. A. Mirkin, and C. Liu, "A modular microfluidic architecture for integrated biochemical analysis," *Proc. Nat. Acad. Sci. USA*, vol. 102, no. 28, pp. 9745–9750, Jul. 2005, doi: [10.1073/pnas.0504082102](https://doi.org/10.1073/pnas.0504082102).
- [11] A. Egatz-Gomez, C. Wang, F. Klacsmann, Z. Pan, S. Marczak, Y. Wang, G. Sun, S. Senapati, and H.-C. Chang, "Future microfluidic and nanofluidic modular platforms for nucleic acid liquid biopsy in precision medicine," *Biomicrofluidics*, vol. 10, no. 3, May 2016, Art. no. 032902, doi: [10.1063/1.4948525](https://doi.org/10.1063/1.4948525).
- [12] Y. Fintschenko, "Education: A modular approach to microfluidics in the teaching laboratory," *Lab Chip*, vol. 11, no. 20, pp. 3394–3400, 2011, doi: [10.1039/C1LC90069B](https://doi.org/10.1039/C1LC90069B).
- [13] S. M. Langelier, E. Livak-Dahl, A. J. Manzo, B. N. Johnson, N. G. Walter, and M. A. Burns, "Flexible casting of modular self-aligning microfluidic assembly blocks," *Lab Chip*, vol. 11, no. 9, pp. 1679–1687, May 2011, doi: [10.1039/C0LC00517G](https://doi.org/10.1039/C0LC00517G).
- [14] J. Nie, Q. Gao, J.-J. Qiu, M. Sun, A. Liu, L. Shao, J.-Z. Fu, P. Zhao, and Y. He, "3D printed Lego-like modular microfluidic devices based on capillary driving," *Biofabrication*, vol. 10, no. 3, Mar. 2018, Art. no. 035001, doi: [10.1088/1758-5090/aaadd3](https://doi.org/10.1088/1758-5090/aaadd3).
- [15] K. C. Bhargava, B. Thompson, and N. Malmstadt, "Discrete elements for 3D microfluidics," *Proc. Nat. Acad. Sci. USA*, vol. 111, no. 42, pp. 15013–15018, Oct. 2014, doi: [10.1073/pnas.1414764111](https://doi.org/10.1073/pnas.1414764111).
- [16] P. K. Yuen, J. T. Bliss, C. C. Thompson, and R. C. Peterson, "Multidimensional modular microfluidic system," *Lab Chip*, vol. 9, no. 22, pp. 3303–3305, Nov. 2009, doi: [10.1039/B912295H](https://doi.org/10.1039/B912295H).
- [17] X. Lai, Z. Shi, Z. Pu, P. Zhang, X. Zhang, H. Yu, and D. Li, "A Rubik's microfluidic cube," *Microsyst. Nanoeng.*, vol. 6, no. 1, pp. 1–12, Jun. 2020, doi: [10.1038/s41378-020-0136-4](https://doi.org/10.1038/s41378-020-0136-4).
- [18] L. J. Y. Ong, T. Ching, L. H. Chong, S. Arora, H. Li, M. Hashimoto, R. DasGupta, P. K. Yuen, and Y.-C. Toh, "Self-aligning Tetris-like (TILE) modular microfluidic platform for mimicking multi-organ interactions," *Lab Chip*, vol. 19, no. 13, pp. 2178–2191, Jun. 2019, doi: [10.1039/C9LC00160C](https://doi.org/10.1039/C9LC00160C).
- [19] P. Loskill, S. G. Marcus, A. Mathur, W. M. Reese, and K. E. Healy, "Organo: A Lego-like plug & play system for modular multi-organ-chips," *PLoS ONE*, vol. 10, no. 10, Oct. 2015, Art. no. e0139587, doi: [10.1371/journal.pone.0139587](https://doi.org/10.1371/journal.pone.0139587).
- [20] S. Dekker, W. Buesink, M. Blom, M. Alessio, N. Verplanck, M. Hihoud, C. Dehan, W. César, A. Le Nel, A. van den Berg, and M. Odijk, "Standardized and modular microfluidic platform for fast lab on chip system development," *Sens. Actuators B, Chem.*, vol. 272, pp. 468–478, Nov. 2018, doi: [10.1016/j.snb.2018.04.005](https://doi.org/10.1016/j.snb.2018.04.005).
- [21] Y.-F. Hsieh, A.-S. Yang, J.-W. Chen, S.-K. Liao, T.-W. Su, S.-H. Yeh, P.-J. Chen, and P.-H. Chen, "A Lego-like swappable fluidic module for bio-chem applications," *Sens. Actuators B, Chem.*, vol. 204, pp. 489–496, Dec. 2014, doi: [10.1016/j.snb.2014.07.122](https://doi.org/10.1016/j.snb.2014.07.122).
- [22] Q. Ji, J. M. Zhang, Y. Liu, X. Li, P. Lv, D. Jin, and H. Duan, "A modular microfluidic device via multimaterial 3D printing for emulsion generation," *Sci. Rep.*, vol. 8, no. 1, pp. 1–10, Mar. 2018, doi: [10.1038/s41598-018-22756-1](https://doi.org/10.1038/s41598-018-22756-1).
- [23] R. Song, M. S. Abbasi, and J. Lee, "Fabrication of 3D printed modular microfluidic system for generating and manipulating complex emulsion droplets," *Microfluidics Nanofluidics*, vol. 23, no. 7, p. 92, Jun. 2019, doi: [10.1007/s10404-019-2258-2](https://doi.org/10.1007/s10404-019-2258-2).
- [24] P. K. Yuen, "A reconfigurable stick-n-play modular microfluidic system using magnetic interconnects," *Lab Chip*, vol. 16, no. 19, pp. 3700–3707, 2016, doi: [10.1039/C6LC00741D](https://doi.org/10.1039/C6LC00741D).
- [25] P. K. Yuen, "SmartBuild—A truly plug-n-play modular microfluidic system," *Lab Chip*, vol. 8, no. 8, pp. 1374–1378, Jul. 2008, doi: [10.1039/B805086D](https://doi.org/10.1039/B805086D).
- [26] P. Gimenez-Gomez, C. Fernandez-Sanchez, and A. Baldi, "Microfluidic modules with integrated solid-state sensors for reconfigurable miniaturized analysis systems," *ACS Omega*, vol. 4, no. 4, pp. 6192–6198, Apr. 2019, doi: [10.1021/acsomega.9b00064](https://doi.org/10.1021/acsomega.9b00064).
- [27] R. Ecker, A. Fuchsluger, and B. Jakoby, "Electroosmotic pump using a glass fiber filter for high flow rate water transport," in *Proc. IEEE Sensors*, Oct. 2021, pp. 1–4, doi: [10.1109/SENSOR547087.2021.9639725](https://doi.org/10.1109/SENSOR547087.2021.9639725).
- [28] R. Mukhopadhyay, "When PDMS isn't the best," *Anal. Chem.*, vol. 79, no. 9, pp. 3248–3253, May 2007, doi: [10.1021/ac071903e](https://doi.org/10.1021/ac071903e).
- [29] R. Ecker, M. Langwiesner, T. Mitteramskogler, A. Fuchsluger, M. A. Hintermüller, and B. Jakoby, "Modular microfluidic PDMS blocks using a magnetic connection system," in *Proc. IEEE Sensors*, Oct. 2022, pp. 1–4, doi: [10.1109/SENSOR552175.2022.9967037](https://doi.org/10.1109/SENSOR552175.2022.9967037).
- [30] V. Saggiomo and A. H. Velders, "Simple 3D printed scaffold-removal method for the fabrication of intricate microfluidic devices," *Adv. Sci.*, vol. 2, no. 9, Sep. 2015, Art. no. 1500125, doi: [10.1002/advs.201500125](https://doi.org/10.1002/advs.201500125).
- [31] A. Stavarakis. (Sep. 2022). *Laminar Flow and Capillary Flow in Microfluidic Chips*. Elveflow. Accessed: Feb. 23, 2023. [Online]. Available: <https://www.elveflow.com/microfluidic-reviews/general-microfluidics/laminar-flow-capillary-flow/>
- [32] P. Agnihotri, "Analysis of interfacial mixing zone and mixing index in microfluidic channels," *Microfluidics Nanofluidics*, vol. 27, no. 2, p. 12, Jan. 2023, doi: [10.1007/s10404-022-02618-z](https://doi.org/10.1007/s10404-022-02618-z).
- [33] D. Stith, "The Tesla valve—A fluidic diode," *Phys. Teacher*, vol. 57, no. 3, p. 201, Mar. 2019, doi: [10.1119/1.5092491](https://doi.org/10.1119/1.5092491).



RAFAEL ECKER (Member, IEEE) received the B.Sc. and Dipl.-Ing. (M.Sc.) degrees from Johannes Kepler University, in 2018 and 2019, respectively, where he is currently pursuing the Ph.D. degree with the Institute of Microelectronics and Microsensors. He is also an University Assistant with Johannes Kepler University. His research interests include the design and fabrication of microfluidic actuators and sensors. He joined the IEEE, in 2019, where he is a member of the Executive Committee of the IEEE Student Branch of the Johannes Kepler University Linz since then.



TINA MITTERAMSKOGLER (Member, IEEE) received the master's degree in physics from KU Leuven, in 2017. She is currently pursuing the Ph.D. degree with the Institute of Microelectronics and Microsensors, Johannes Kepler University Linz. She is also an University Assistant with Johannes Kepler University Linz. Her research interest includes the behavior of liquids in open and microchannels. She joined IEEE, in 2021, where she is also a part of the Executive Committee of IEEE Student Branch of Johannes Kepler University Linz since then.



MANUEL LANGWIESNER was born in Amstetten, Austria, in 1997. He received the B.Sc. degree in mechatronics from Johannes Kepler University Linz, Linz, Austria, in 2022, where he is currently pursuing the M.Sc. degree in mechatronics. His research interests include signals processing, measurement technology, and electronics.



ANDREAS FUCHSLUGER (Member, IEEE) received the Mag. rer. nat. degree in mathematics and physics and the Dipl.-Ing. (M.Sc.) degree in technical physics, in 2018 and 2021, respectively. He is currently pursuing the Ph.D. degree with the Institute for Microelectronics and Microsensors, Johannes Kepler University Linz. His research interest includes microfluidics with the focus on acoustofluidics. He joined IEEE, in 2021. He is the Chair of the IEEE Student Branch Linz.



MARCUS A. HINTERMÜLLER was born in Linz, Austria, in 1990. He received the Dipl.-Ing. (M.Sc.) degree in mechatronics engineering and the Ph.D. degree in technical sciences from Johannes Kepler University Linz, Austria, in 2016 and 2021, respectively. From 2016 to 2021, he was an University Assistant with the Institute for Microelectronics and Microsensors, Johannes Kepler University Linz. His research interests include the modeling and experimental investigation of microfluidic effects and sensor integration in microfluidic devices.



BERNHARD JAKOBY (Fellow, IEEE) received the Dipl.-Ing. (M.Sc.) degree in communication engineering, the Ph.D. degree in electrical engineering, and the Venia Legendi degree in theoretical electrical engineering from the Vienna University of Technology (VUT), Austria, in 1991, 1994, and 2001, respectively.

From 1991 to 1994, he was a Research Assistant with the Institute of General Electrical Engineering and Electronics, VUT. He stayed as an Erwin Schrödinger Fellow with the University of Ghent, Belgium, performing research on the electrodynamics of complex media. From 1996 to 1999, he was a Research Associate and later an Assistant Professor with the Delft University of Technology, The Netherlands, working in the field of microacoustic sensors. From 1999 to 2001, he was with the Automotive Electronics Division, Robert Bosch GmbH, Germany, where he was conducting development projects in the field of automotive liquid sensors. He joined the newly formed Industrial Sensor Systems Group, VUT, as an Associate Professor, in 2001. He was appointed as a Full Professor in microelectronics with Johannes Kepler University, Linz, Austria, in 2005, where he is currently working in the field of sensors. He was elected as a Eurosenors Fellow, in 2009. He received the Outstanding Paper Award 2010 for a paper in the IEEE TRANSACTIONS ON ULTRASONICS, FERROELECTRICS, AND FREQUENCY CONTROL. He is a Full Member of the Austrian Academy of Sciences. He served as the Technical Co-Chair, the Co-Chair, and the General Chair for various conferences, including the IEEE Sensors Conference and the I2MTC. He is also an Editorial Board Member of the IEEE SENSORS JOURNAL and *Measurement Science and Technology*.

...